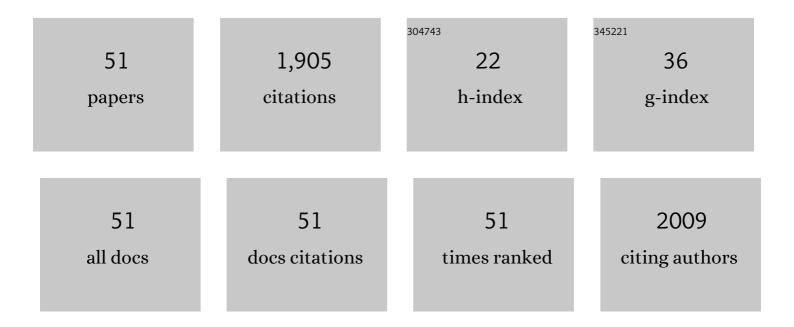
Kimmo Rautiainen

List of Publications by Year in descending order

Source: https://exaly.com/author-pdf/7334609/publications.pdf Version: 2024-02-01



#	Article	IF	CITATIONS
1	Freeze–Thaw Detection Over High-Latitude Regions by Means of GNSS-R Data. IEEE Transactions on Geoscience and Remote Sensing, 2022, 60, 1-13.	6.3	12
2	Effects of Arctic Wetland Dynamics on Tower-Based GNSS Reflectometry Observations. IEEE Transactions on Geoscience and Remote Sensing, 2022, 60, 1-17.	6.3	3
3	Overview: Recent advances in the understanding of the northern Eurasian environments and of the urban air quality in China – a Pan-Eurasian Experiment (PEEX) programme perspective. Atmospheric Chemistry and Physics, 2022, 22, 4413-4469.	4.9	9
4	Daily High-Resolution Land Surface Freeze/Thaw Detection Using Sentinel-1 and AMSR2 Data. Remote Sensing, 2022, 14, 2854.	4.0	0
5	An Introduction to the HydroCNSS GNSS Reflectometry Remote Sensing Mission. IEEE Journal of Selected Topics in Applied Earth Observations and Remote Sensing, 2021, 14, 6987-6999.	4.9	46
6	Sentinel-1 based soil freeze/thaw estimation in boreal forest environments. Remote Sensing of Environment, 2021, 254, 112267.	11.0	10
7	Temperature effects on L-band vegetation optical depth of a boreal forest. Remote Sensing of Environment, 2021, 263, 112542.	11.0	12
8	GNSS-Reflected Signals for Permafrost Monitoring. , 2021, , .		1
9	Utilizing Earth Observations of Soil Freeze/Thaw Data and Atmospheric Concentrations to Estimate Cold Season Methane Emissions in the Northern High Latitudes. Remote Sensing, 2021, 13, 5059.	4.0	5
10	Spaceâ€Based Observations for Understanding Changes in the Arcticâ€Boreal Zone. Reviews of Geophysics, 2020, 58, e2019RG000652.	23.0	39
11	SodSAR: A Tower-Based 1–10 GHz SAR System for Snow, Soil and Vegetation Studies. Sensors, 2020, 20, 6702.	3.8	6
12	Refurbishment of the HUTRAD system. , 2020, , .		0
13	A Modeling-Based Approach for Soil Frost Detection in the Northern Boreal Forest Region With C-Band SAR. IEEE Transactions on Geoscience and Remote Sensing, 2019, 57, 1069-1083.	6.3	14
14	Validation of the SMAP freeze/thaw product using categorical triple collocation. Remote Sensing of Environment, 2018, 205, 329-337.	11.0	27
15	GNSS Transpolar Earth Reflectometry exploriNg System (G-TERN): Mission Concept. IEEE Access, 2018, 6, 13980-14018.	4.2	55
16	Season -Length Observations of Active and Passive Microwave Signatures of Snow Cover in a Boreal Forest Environment. , 2018, , .		2
17	Soil Permittivity and Soil Frost Retrievals Using a Synergistic Method for Active and Passive Microwave Instruments. , 2018, , .		0
18	Spatially Distributed Evaluation of ESA CCI Soil Moisture Products in a Northern Boreal Forest Environment. Geosciences (Switzerland), 2018, 8, 51.	2.2	16

KIMMO RAUTIAINEN

#	Article	IF	CITATIONS
19	Proxy Indicators for Mapping the End of the Vegetation Active Period in Boreal Forests Inferred from Satellite-Observed Soil Freeze and ERA-Interim Reanalysis Air Temperature. PFG - Journal of Photogrammetry, Remote Sensing and Geoinformation Science, 2018, 86, 169-185.	1.1	1
20	Validation of SMAP surface soil moisture products with core validation sites. Remote Sensing of Environment, 2017, 191, 215-231.	11.0	503
21	Retrieving landscape freeze/thaw state from Soil Moisture Active Passive (SMAP) radar and radiometer measurements. Remote Sensing of Environment, 2017, 194, 48-62.	11.0	113
22	Nordic Snow Radar Experiment. Geoscientific Instrumentation, Methods and Data Systems, 2016, 5, 403-415.	1.6	37
23	The Sodankylän situ soil moisture observation network: an example application of ESAÂCCI soil moisture product evaluation. Geoscientific Instrumentation, Methods and Data Systems, 2016, 5, 95-108.	1.6	28
24	Soil moisture sensor calibration for organic soil surface layers. Geoscientific Instrumentation, Methods and Data Systems, 2016, 5, 109-125.	1.6	32
25	SMOS prototype algorithm for detecting autumn soil freezing. Remote Sensing of Environment, 2016, 180, 346-360.	11.0	109
26	Retrieval of snow parameters from L-band observations - application for SMOS and SMAP. , 2016, , .		4
27	Snow density and ground permittivity retrieved from L-band radiometry: Application to experimental data. Remote Sensing of Environment, 2016, 180, 377-391.	11.0	60
28	ESA's Soil Moisture and Ocean Salinity mission: From science to operational applications. Remote Sensing of Environment, 2016, 180, 3-18.	11.0	77
29	Potential of L-band passive microwave radiometry for snow parameter retrieval. , 2015, , .		0
30	Effects of Meteorological and Ancillary Data, Temporal Averaging, and Evaluation Methods on Model Performance and Uncertainty in a Land Surface Model. Journal of Hydrometeorology, 2015, 16, 2559-2576.	1.9	22
31	Snow Density and Ground Permittivity Retrieved from L-Band Radiometry: A Synthetic Analysis. IEEE Journal of Selected Topics in Applied Earth Observations and Remote Sensing, 2015, 8, 3833-3845.	4.9	59
32	Simulating seasonally and spatially varying snow cover brightness temperature using HUT snow emission model and retrieval of a microwave effective grain size. Remote Sensing of Environment, 2015, 156, 71-95.	11.0	37
33	Detection of soil freezing from L-band passive microwave observations. Remote Sensing of Environment, 2014, 147, 206-218.	11.0	120
34	Model for microwave emission of a snow-covered ground with focus on L band. Remote Sensing of Environment, 2014, 154, 180-191.	11.0	62
35	L-Band Radiometer Observations of Soil Processes in Boreal and Subarctic Environments. IEEE Transactions on Geoscience and Remote Sensing, 2012, 50, 1483-1497.	6.3	106
36	Experimental Study on Radiometric Performance of Synthetic Aperture Radiometer HUT-2D—Measurements of Natural Targets. IEEE Transactions on Geoscience and Remote Sensing, 2011, 49, 814-826.	6.3	16

#	Article	IF	CITATIONS
37	Detection of a Sea Surface Salinity Gradient Using Data Sets of Airborne Synthetic Aperture Radiometer HUT-2-D and a GNSS-R Instrument. IEEE Transactions on Geoscience and Remote Sensing, 2011, 49, 4561-4571.	6.3	4
38	Synthetic aperture radiometer measurements of freezing soil. , 2011, , .		0
39	Investigation of Radio Frequency Interference at L-band using data from airborne HUT-2D radiometer and spaceborne SMOS radiometer. , 2011, , .		2
40	Lessons learned from HUT-2D L-band airborne demonstrator. , 2011, , .		1
41	L-band measurements of boreal soil. , 2010, , .		3
42	Experimental study on radiometric performance of synthetic aperture radiometer hut-2D – Measurements of natural targets. , 2010, , .		0
43	Soil moisture retrieval from HUT-2D synthetic aperture radiometer data. , 2009, , .		0
44	Error Propagation in Calibration Networks of Synthetic Aperture Radiometers. IEEE Transactions on Geoscience and Remote Sensing, 2009, 47, 3140-3150.	6.3	3
45	Sea surface salinity retrieval demonstration using datasets of synthetic aperture radiometer HUT-2D. , 2009, , .		1
46	Helsinki University of Technology L-Band Airborne Synthetic Aperture Radiometer. IEEE Transactions on Geoscience and Remote Sensing, 2008, 46, 717-726.	6.3	60
47	Ground calibration of SMOS: NIR and CAS. , 2007, , .		4
48	SMOS Calibration Subsystem. IEEE Transactions on Geoscience and Remote Sensing, 2007, 45, 3691-3700.	6.3	31
49	First 2-D Interferometric Radiometer Imaging of the Earth From an Aircraft. IEEE Geoscience and Remote Sensing Letters, 2007, 4, 241-245.	3.1	34
50	MIRAS end-to-end calibration: application to SMOS L1 processor. IEEE Transactions on Geoscience and Remote Sensing, 2005, 43, 1126-1134.	6.3	91
51	Analysis of correlation and total power radiometer front-ends using noise waves. IEEE Transactions on Geoscience and Remote Sensing, 2005, 43, 2452-2459.	6.3	28